Supplementary Materials for

Behaviorally-selective engagement of short-latency effector pathways by motor cortex

Andrew Miri, Claire L. Warriner, Jeffrey S. Seely, Gamaleldin F. Elsayed

John P. Cunningham, Mark M. Churchland and Thomas M. Jessell

A

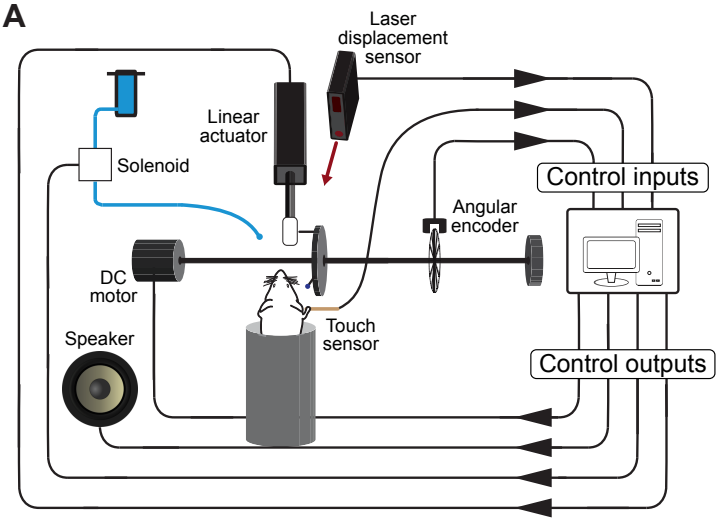

B

Training timeline

Day 1	Begin water schedule
Day 5-6	Begin handling by experimenter
Day 7-8	Acclimate to head fixation
Day 9	Begin shaping wheel rotation
~Day 14	Begin shaping reach to joystick, pull
~Day 21	Reach distance reaches full length
~Day 24	Begin recording or inactivation

C

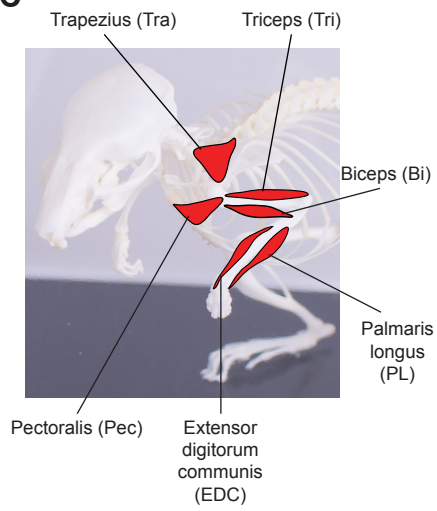

D

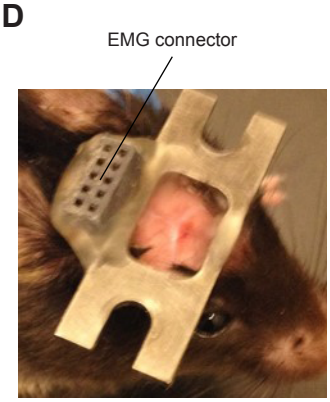

E

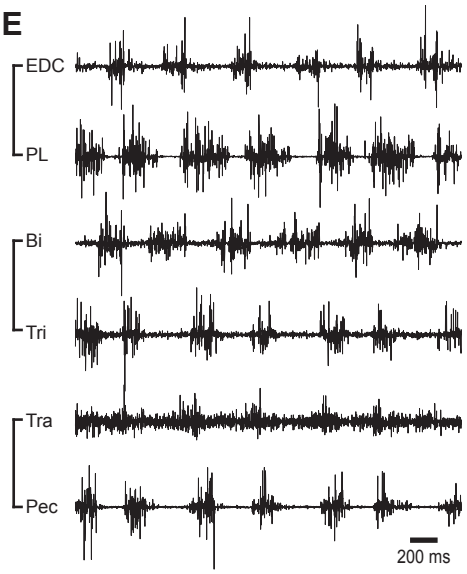

F

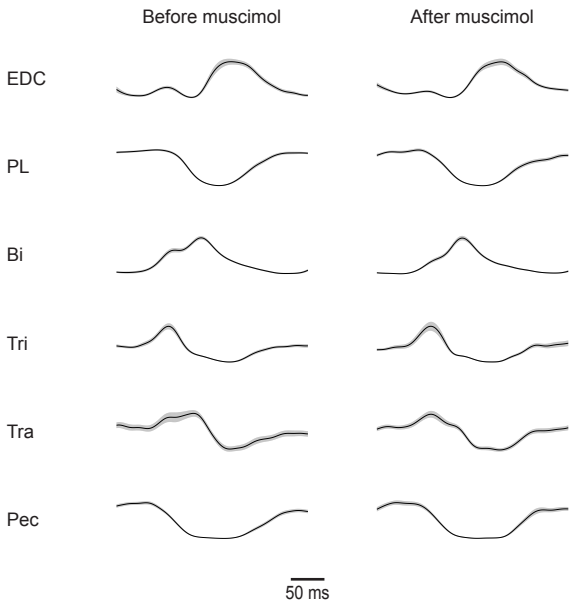

G

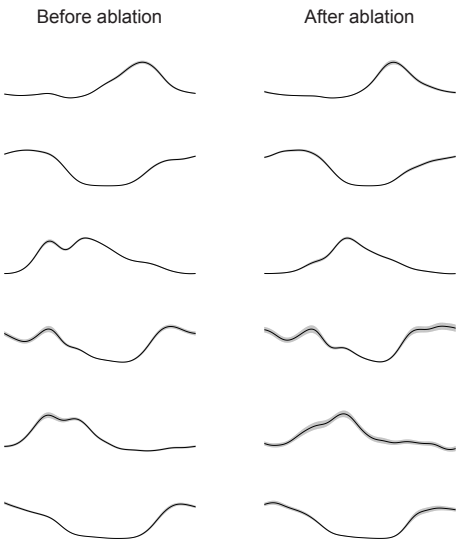

Figure S1: Behavior and EMG recording; related to Figure 1

(A) Schematic depicting the paradigm in which mice are trained to perform the precision pull behavior. (B) Approximate timeline for precision pull training. (C) Schematic depicting the six forelimb muscles from which EMG was recorded. (D) Photograph displaying the EMG connector affixed to the headplate on an experimental animal. (E) Example EMG recordings from the muscles shown in (C) during treadmill walking. (F),(G) Trial-averaged EMG (black) ± SEM (gray) recorded during treadmill walking before (left) and after (right) unilateral muscimol injection into (F) or ablation of (G) the caudal forelimb area. The similarity between locomotor behavior before and after motor cortical inactivation with muscimol or tissue ablation was observed in two mice walking at 20 cm/s.

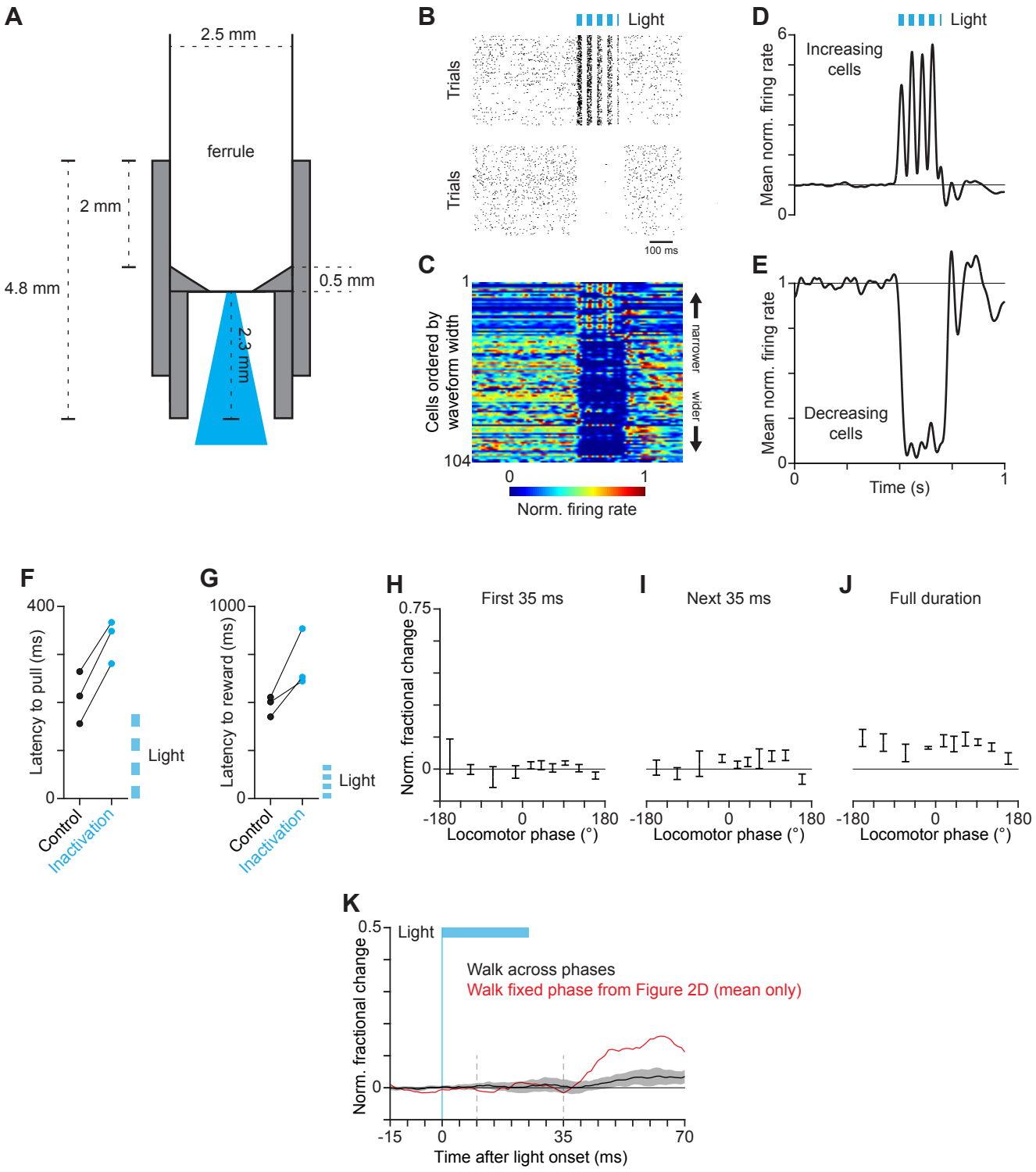
A
2.5 mm
ferrule
2 mm
4.8 mm
0.5 mm
2.3 mm
B
Light
Trials
Trials
100 ms
C
Cells ordered by waveform width
1
104
narrower
wider
0
1
Norm. firing rate
D
Light
Increasing cells
Mean norm. firing rate
6
0
E
Mean norm. firing rate
1
0
Decreasing cells
0
1
Time (s)
F
Latency to pull (ms)
400
0
Light
Control
Inactivation
G
Latency to reward (ms)
1000
0
Light
Control
Inactivation
H
First 35 ms
Norm. fractional change
0.75
0
-180
0
180
Locomotor phase (°)
I
Next 35 ms
-180
0
180
Locomotor phase (°)
J
Full duration
-180
0
180
Locomotor phase (°)
K
Norm. fractional change
0.5
0
Light
Walk across phases
Walk fixed phase from Figure 2D (mean only)
-15
0
35
70
Time after light onset (ms)

Figure S2: Fast timescale inactivation of forelimb motor cortex; related to Figure 2

(A) Schematic depicting the stainless steel ferrule guide positioned above the cortical surface by cementing it to the headplate. Ferrule guides enabled quick and reliable positioning of an optical patch cable's ferrule above the brain surface. (B) Spike rasters for individual neurons that increase (top) and decrease (bottom) their firing during motor cortical inactivation in *VGAT-ChR2-EYFP* mice. Blue bars above (B) and (D) depict the timing of light stimulation. Data in (B)-(E) were collected during head fixation but not during precision pull behavior. (C) Normalized trial-averaged firing rates during blue light stimulation for 104 neurons recorded in two different mice, sorted by spike waveform width. Narrow waveforms should correspond primarily to fast-spiking interneurons, which we expect to express ChR2 and be activated, while longer waveforms should correspond primarily to pyramidal neurons that we expect should not express ChR2. (D),(E) Mean normalized firing rates during blue light stimulation across neurons that increased (D) and decreased (E) their firing in response. Here, trial-averaged firing rates were averaged across neurons and then normalized by their mean value 500 to 200 ms prior to blue light stimulation. The smoothing of firing rates with a 10 ms Gaussian gives the illusion that responses slightly precede stimulus onset. (F),(G) Mean latency to pull (F) or latency to reward (G) for trials without (black, Control) or with (blue, Inactivation) stimulation triggered on reach initiation (3 mice). (H)-(J) Mean ± SEM normalized fractional change in muscle activity between control and inactivation trials summed over the first 35 ms (H), the subsequent 35 ms (I), or the entire duration (J) of light stimulation, as a function of the locomotor phase at which stimulation began. Trials were grouped according to the phase of stimulation onset, and data are plotted along the x axis according to the mean onset phase for each group. Change measurements were squared (see Methods), so values fall below zero compared to control changes only by chance. (K) Mean ± SEM normalized

fractional change in muscle activity between control and inactivation initiated at random phases during treadmill walking (gray). Overlaid for comparison is the mean for inactivation at a single fixed phase shown in Figure 2D (red). Vertical dotted lines are drawn at 10 and 35 ms after light onset.

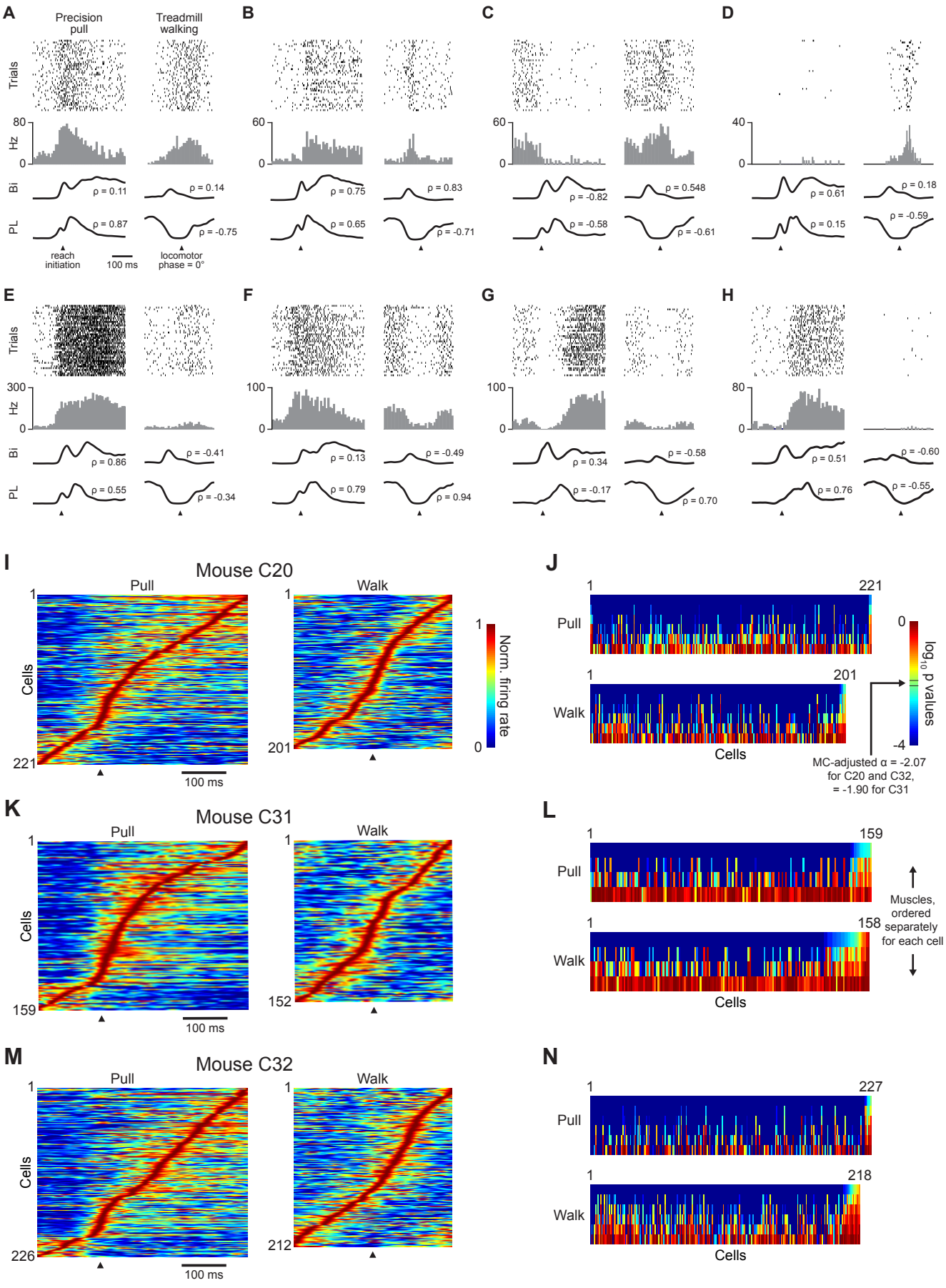
A
Precision pull
Treadmill walking
Trials
Hz
Bi
PL
ρ = 0.11
ρ = 0.14
ρ = 0.87
ρ = -0.75
reach initiation
100 ms
locomotor phase = 0°
B
ρ = 0.75
ρ = 0.83
ρ = 0.65
ρ = -0.71
C
ρ = -0.82
ρ = 0.548
ρ = -0.58
ρ = -0.61
D
ρ = 0.61
ρ = 0.18
ρ = 0.15
ρ = -0.59
E
ρ = 0.86
ρ = -0.41
ρ = 0.55
ρ = -0.34
F
ρ = 0.13
ρ = -0.49
ρ = 0.79
ρ = 0.94
G
ρ = 0.34
ρ = -0.58
ρ = -0.17
ρ = 0.70
H
ρ = 0.51
ρ = -0.60
ρ = 0.76
ρ = -0.55
I
Mouse C20
Pull
Walk
Cells
Norm. firing rate
100 ms
J
Pull
Walk
Cells
log10 p values
MC-adjusted α = -2.07
for C20 and C32,
= -1.90 for C31
K
Mouse C31
L
Muscles, ordered separately for each cell
M
Mouse C32
N

Figure S3: Neural recording during reaching and walking; related to Figure 4

(A)-(H) Spike rasters and histograms (top) for the neurons whose trial averaged firing rates are depicted in Figure 4B, together with the trial-averaged activation of biceps (Bi) and palmaris longus (PL). The arrangement of cells follows that in Figure 4B. Pearson correlation scores (ρ) are given for the correlation of each muscle activity time series with the corresponding neuronal firing rate. (I),(K),(M) Normalized trial-averaged neuronal firing rates with means > 1 Hz that are significantly correlated with the activity of at least one muscle during precision pull (left) and treadmill walking (right). Each panel shows results from a different mouse. (J),(L),(N) Matrices of $\log_{10}$ p values resulting from testing the significance of the correlation between neuronal firing rates and the activation of individual muscles for neurons with mean rates > 1 Hz during precision pull (top) and treadmill walking (bottom). Values are in ascending order for each neuron, and consequently each row does not correspond to values for an individual muscle. The nearly uniformly low p values in the top row of each matrix illustrate the large fraction of neurons whose firing rates were significantly correlated with the activity of at least one muscle. Each panel shows results from a different mouse. The p value thresholds (α) indicated on the scale bar were adjusted for multiple comparisons using a false discovery rate-based correction.

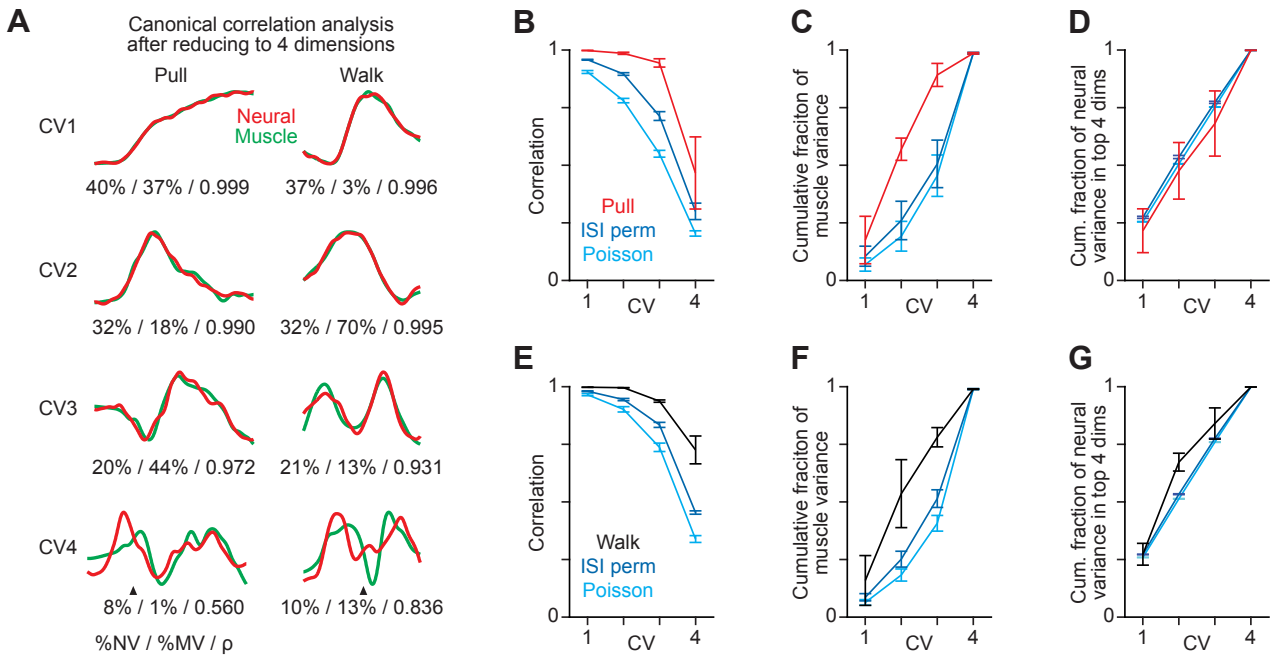
A
Canonical correlation analysis
after reducing to 4 dimensions
Pull
Walk
CV1
Neural
Muscle
40% / 37% / 0.999
37% / 3% / 0.996
CV2
32% / 18% / 0.990
32% / 70% / 0.995
CV3
20% / 44% / 0.972
21% / 13% / 0.931
CV4
8% / 1% / 0.560
10% / 13% / 0.836
%NV / %MV / ρ
B
Correlation
Pull
ISI perm
Poisson
CV
C
Cumulative fraciton of muscle variance
D
Cum. fraction of neural variance in top 4 dims
E
Walk
F
G

Figure S4: Muscle-correlated motor cortical firing during precision pull and treadmill walking; related to Figure 4

To quantify the similarity between neuronal firing and muscle activity, we used canonical correlation analysis to compare the set of trial-averaged neural firing rates with the set of trial-averaged muscle activations from individual mice. We first reduced the neural and muscle data each to four dimensions (variance explained, neural: pull 95 ± 1%, walk 90 ± 0.3%; muscle: pull 99 ± 0.3%, walk 99 ± 0.2%) and applied a temporal offset that maximized similarity between neural and muscle data. Comparable results were found using a newly developed CCA variant in which canonical variables are constrained to form orthogonal sets (Cunningham and Ghahramani, 2015). (A) Results from canonical correlation analysis of the set of neuronal firing rates and the set of muscle activations from one mouse for both pull (left) and walk (right). NV = neural variance captured; MV = muscle variance captured; ρ = Pearson correlation. (B)-(D) Mean ± SEM correlation between (B), cumulative muscle variance explained by (C), and cumulative neural variance for the first 4 activity dimensions explained by (D) the canonical variables resulting from canonical correlation analysis on activity during pull (red), on pull activity with permuted interspike intervals (blue), and on pull activity with neurons replaced by simulated Poisson neurons having an identical firing rate distribution (cyan). (E)-(G) Same as (B)-(D), but for activity measured during walking.

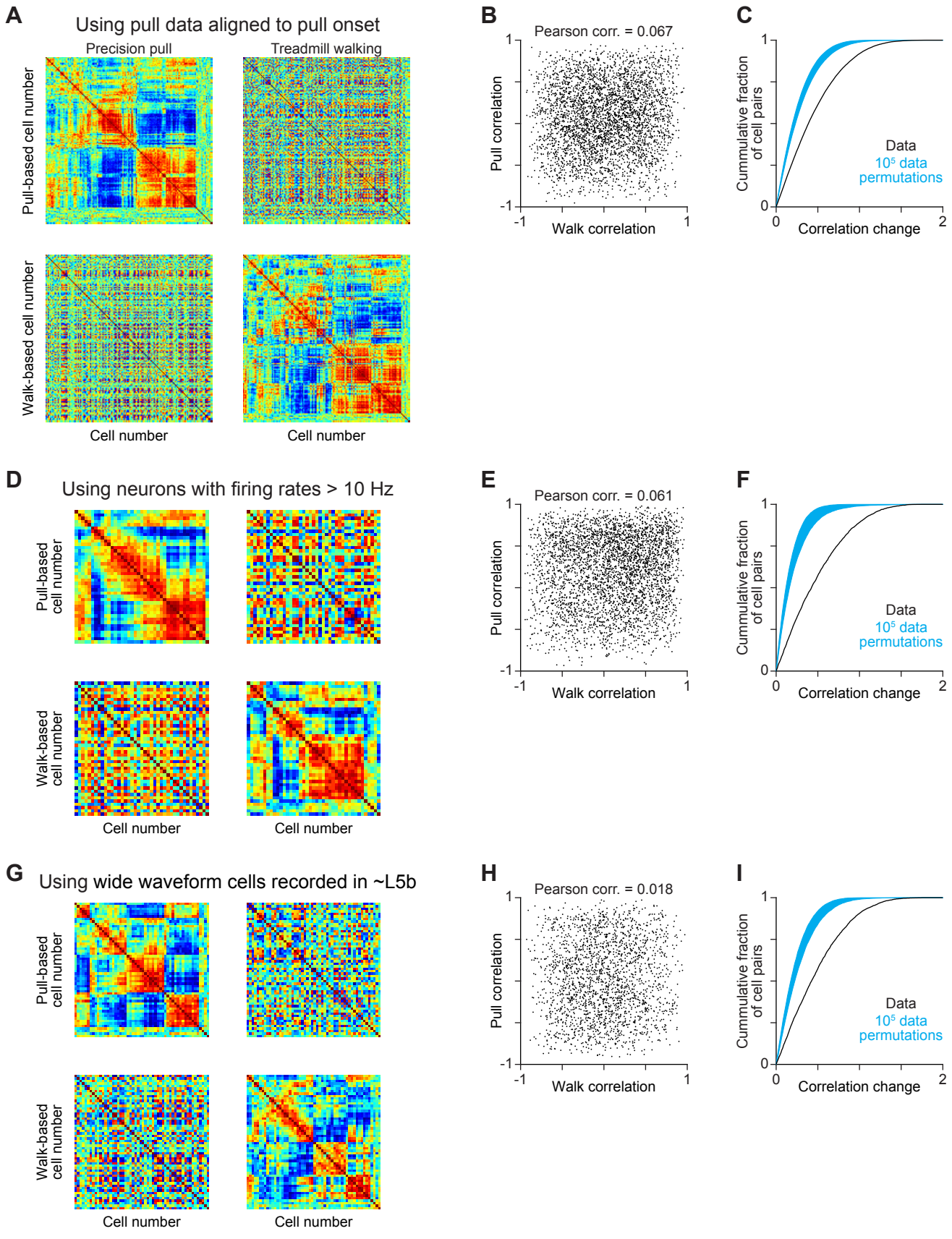
A
Using pull data aligned to pull onset
Precision pull
Treadmill walking
Pull-based cell number
Walk-based cell number
Cell number
Cell number
B
Pearson corr. = 0.067
Pull correlation
Walk correlation
C
Cummulative fraction of cell pairs
Data
10⁵ data permutations
Correlation change
D
Using neurons with firing rates > 10 Hz
Pull-based cell number
Walk-based cell number
Cell number
Cell number
E
Pearson corr. = 0.061
Pull correlation
Walk correlation
F
Cummulative fraction of cell pairs
Data
10⁵ data permutations
Correlation change
G
Using wide waveform cells recorded in ~L5b
Pull-based cell number
Walk-based cell number
Cell number
Cell number
H
Pearson corr. = 0.018
Pull correlation
Walk correlation
I
Cummulative fraction of cell pairs
Data
10⁵ data permutations
Correlation change

Figure S5: Changes in the correlation of neuronal firing rates between behaviors; related to Figure 6

(A) Matrices of correlation scores for neuronal firing in one mouse during the precision pull task (left column) and treadmill walking (right column) ordered to cluster together neurons with similar correlation patterns during pull (top row) and walk (bottom row) constructed using pull trials aligned to pull onset. (B) Correlation between the firing rates of pairs of neurons during pull plotted versus their correlation during walk using pull trials aligned to pull onset. Every tenth data point is plotted from three mice. (C) Cumulative histogram for the change in pairwise firing rate correlations between behaviors (black) and 100,000 iterations of the same histogram calculated after data permutation (cyan) using pull trials aligned to pull onset. (D) Matrices of correlation scores for neuronal firing in one mouse constructed using neurons with mean firing rates > 10 Hz during both behaviors. For (D)-(I), pull trials were aligned to reach onset, as in Figure 6C. (E) Correlation between the firing rates of pairs of neurons during pull plotted versus their correlation during walk for neurons with mean firing rates > 10 Hz during both behaviors (3 mice). (F) Cumulative histogram for the change in pairwise firing rate correlations between behaviors (black) and 100,000 iterations of the same histogram calculated after data permutation (cyan) for neurons with mean firing rates > 10 Hz during both behaviors. (G) Matrices of correlation scores for neuronal firing in one mouse constructed using wide-spiking neurons recorded within layer 5b. (H) Correlation between the firing rates of pairs of neurons during pull plotted versus their correlation during walk for wide-spiking neurons recorded within layer 5b (3 mice). (I) Cumulative histogram for the change in pairwise firing rate correlations between behaviors (black) and 100,000 iterations of the same histogram calculated after data permutation (cyan) for wide-spiking neurons recorded within layer 5b.

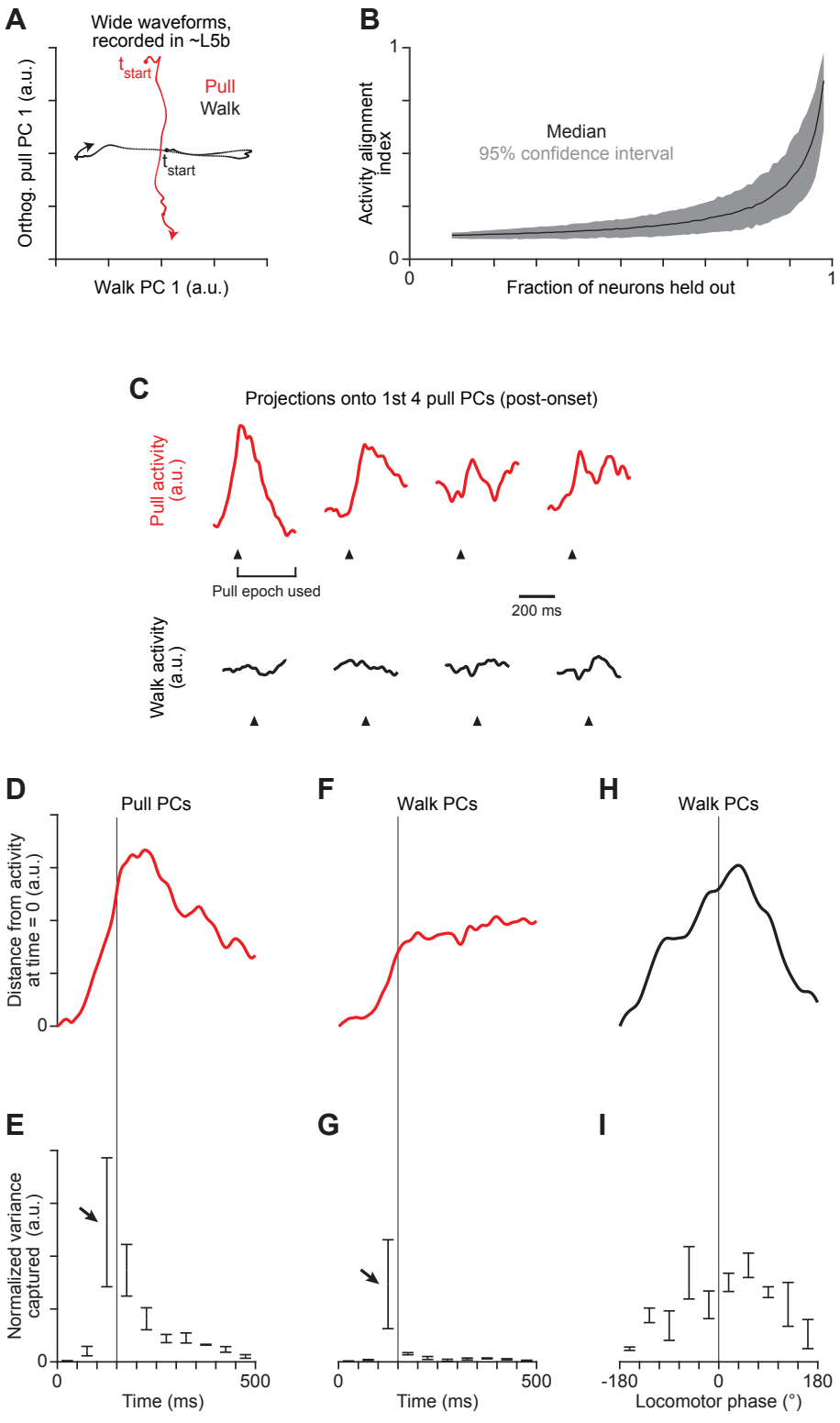
A
Wide waveforms,
recorded in ~L5b
t start
Pull
Walk
t start
Orthog. pull PC 1 (a.u.)
Walk PC 1 (a.u.)
B
Activity alignment index
1
0
Median
95% confidence interval
0
1
Fraction of neurons held out
C
Projections onto 1st 4 pull PCs (post-onset)
Pull activity (a.u.)
Pull epoch used
200 ms
Walk activity (a.u.)
D
Pull PCs
Distance from activity at time = 0 (a.u.)
0
F
Walk PCs
H
Walk PCs
E
Normalized variance captured (a.u.)
0
0
500
Time (ms)
G
0
500
Time (ms)
I
-180
0
180
Locomotor phase (°)

Figure S6: Comparing principal components for pull and walk; related to Figure 7

(A) The relation between the activity of wide-spiking neurons recorded within layer 5b in one mouse during pull (red) and walk (black) projected onto the first principal component for the activities during walk and the first principal component for the activities during pull minus its projection onto the first axis (Orthogonalized). (B) Median (black) and 95% confidence interval (gray) for alignment between neuronal firing rates during pull and walk, after dropping out between 10 and 98% of the population. For a given percentage dropped, alignment indices were computed after dropping each of 1000 different random subsets of neurons. The median and confidence interval were calculated from the 1000 resulting values. (C) Projection of neuronal population activity from one mouse during precision pull (red) and treadmill walking (black) onto the top 4 principal components for the activity following the onset of muscle activation during pull. Arrowheads indicate the time of muscle activation onset during pull, and 0º in phase during the locomotor cycle. (D),(F) Distance of the activity during pull from its position at time = 0 ms within the space comprised by the top 4 principal components for pull (D) or walk (F) for one mouse. Muscle activation onset is indicated by the vertical line at time = 150 ms. (E),(G) Normalized pull variance captured by the top 4 principal components for pull (E) or walk (G) for 10 successive 50 ms intervals. Error bars in (E),(G) and (I) represent mean ± SEM for 3 mice. Values in (E),(G) and (I) are normalized by the total variance for each animal during pull. (H) Distance of the activity during walk from its position at locomotor phase = -180º within the space comprised by the top 4 principal components for walk for one mouse. (I) Normalized walk variance captured by the top 4 principal components for walk for 10 successive 36º intervals.

For each muscle in each animal:

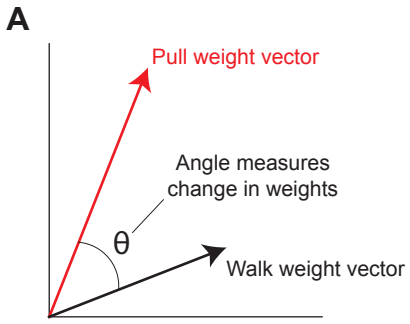

Static model

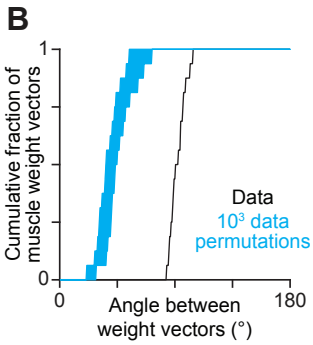

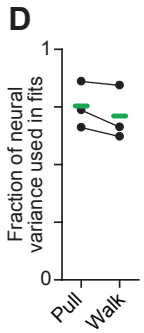

Dynamic model

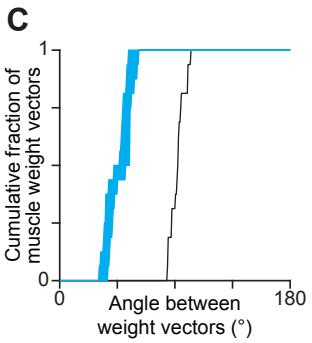

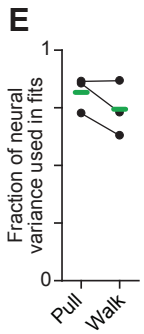

Figure S7: An implication of our findings: the correlations between motor cortical and muscle activity change between behaviors; related to Figure 7

To illustrate this change, we fit linear models of neuronal firing rates to the activity of individual muscles, separately for precision pull and treadmill walking, using ridge regression with cross-validation to compute model weights. To account for a broad range of the ways in which neural and muscle activity can be related, we used two different model types; one in which muscle activity is fit by weighted sums of neural activities ("static"), and another that describes muscle activity as a weighted sum of the outputs of a dynamical system that takes the neural activities as inputs ("dynamic"). For both model types, we found a large change in the magnitude of model weights between behaviors, indicating the change in the pattern of neuron-muscle correlation (static model: median 44.1 standard deviations beyond null distribution median, dynamic model: 43.8; $p < 10^{-3}$, one-tailed Monte Carlo test). This change does not appear to be attributable to a reduction in the overall degree of neuron-muscle correlation, as model fit quality and neural variance used change much less between behaviors (muscle variance captured > 98% in all cases). (A) Schematic of the quantification of fit changes between behaviors. The angle subtended by two weight vectors for fits to a given muscle was used because this is not sensitive to differences between behaviors in the magnitude of muscle activation. Each weight vector has an element for each neuronal firing rate time series used as a regressor in the fit. (B),(C) Cumulative histogram for the change between the weight vectors in static (B) and dynamic (C) regression models of muscle activity during precision pull and treadmill walking (black) and 1000 iterations of the same histogram calculated after data permutation (cyan). (D),(E) Fraction of neural variance used in the static (D) and dynamic (E) regression models. Green bars show the means across 3 mice. Lines connect data points from the same animal.

Movie S1: Mouse performing the precision pull task; related to Figure 1

Video depicts a head-fixed mouse performing the precision pull task. As the video begins, the mouse awaits trial onset with its right paw resting on a rung. The bright spot on the wrist is reflected light from the laser displacement sensor used to enforce proper initial paw position. The trial begins when the joystick is rapidly positioned in front of the mouse. The mouse then executes the precision pull behavior, grasping and then pulling the joystick a set but short distance. The mouse then receives a water reward, and the joystick is moved out of the mouse's reach until the next trial is initiated. Video is $3.\overline{3}$x actual speed.

Movie S2: Mouse walking along treadmill; related to Figure 1

Video depicts a mouse walking along the motor-driven treadmill within a Plexiglas enclosure. Video is $3.\overline{3}$x actual speed.